ARTICLE NO. 79-0359R

.0005
.0001
.0002

J80-052

Model of Transverse Fuel Injection in Supersonic Combustors

R. C. Rogers*
NASA Langley Research Center, Hampton, Va.

A two-dimensional, nonreacting flow model of the aerodynamic interaction of a transverse hydrogen jet within a supersonic mainstream has been developed. The model assumes profile shapes of mass flux, pressure, flow angle, and hydrogen concentration and produces downstream profiles of the other flow parameters under the constraints of the integrated conservation equations. These profiles are used as starting conditions for an existing finite difference parabolic flow computer code for the turbulent supersonic combustion of hydrogen. Integrated mixing and flow profile results obtained from the computer code compare favorably with existing data for the supersonic combustion of hydrogen.

Nomenclature

A_k = constant in Eq. (16), = 0.6935
A_R = constant in Eq. (24), = −10.0
$\bar{c}_F$ = mean skin friction coefficient
C_R = constant in Eq. (24), = −0.15
C_u = profile decay factor defined by Eq. (18)
d = injector diameter
f = ratio of fuel and mainstream mass flow rates
F_w = pressure force on injection wall
F_J = total jet momentum, $=(\rho_f V_f^2 + p_f) A_f$
h = duct height
H = sensible enthalpy plus chemical potential
H° = stagnation enthalpy, $= H + V^2/2$
K = turbulent kinetic energy, Eq. (34)
L_m = mixing length
M = Mach number
p = static pressure
p_b = reference pressure for data
p_B = effective back pressure of the fuel jet, $= 2/3\, p_{t,2}$
$p_{t,2}$ = pitot pressure
$p_{t,f}$ = jet stagnation pressure
q_r = ratio of jet and mainstream dynamic pressure
R = mass flux function, Eq. (24), $\equiv \rho V/(\rho V)_\delta$
S_f = skin friction force, $= \frac{1}{2}\rho_0 V_0^2 \bar{c}_f x_{LG}$
s = injector spacing
T = static temperature and flow angle function in Eq. (28)
T_t = stagnation temperature
V = velocity
x = streamwise coordinate
x_{LG} = total length of model control volume
z, z' = transverse coordinate
Z = nondimensional coordinate, $= z/h_2$
$\hat{Z}$ = nondimensional coordinate in Eq. (17)
α_T, α_B = angles of top and bottom walls of duct
α_f = fuel injection angle
γ = ratio of specific heats
δ = local flow angle
η_m = mixing efficiency parameter
κ = fuel mass fraction
ρ = density
θ = shock angle
μ = molecular weight

Subscripts

0 = mainstream property
2 = solution plane of model
e = duct exit
f = fuel or jet property
L = location of solution plane or property behind shock at the solution plane
m = mean value
s = shock property
sep = separation
w = wall value
δ = edge of the mixing region
κ = local fuel peak concentration

Presented as Paper 79-0359 at the AIAA 17th Aerospace Sciences Meeting, New Orleans, La., Jan. 15-17, 1979; submitted Jan. 29, 1979; revision received Aug. 17, 1979. Reprints of this article may be ordered from AIAA Special Publications, 1290 Avenue of the Americas, New York, N.Y. 10019. Order by Article No. at top of page. Member price $2.00 each, nonmember, $3.00 each. **Remittance must accompany order.**

Index categories: Airbreathing Propulsion; Combustion and Combustor Designs; Computational Methods.

*Aerospace Engineer, Hypersonic Propulsion Branch, High-Speed Aerodynamics Division. Member AIAA.

Introduction

THE injection of fuel transverse to the mainstream flow has been a feature of ramjet combustor designs since their inception. Investigations of the interaction of a transverse jet in a supersonic flow have been primarily interested in the initial penetration and subsequent downstream mixing of the fuel. Because the transverse jet interaction (TJI) flowfield contains shock waves, flow recirculation, and separation zones, which are often three-dimensional, completely analytical solutions require the use of the fully elliptic form of the partial differential equations of motion. These equations for the three-dimensional elliptic flow of the TJI region cannot presently be solved on existing computers because of the large storage and computational times required. Therefore, most results for a transverse jet in a supersonic stream have been empirically derived from experimental observations of the TJI flow.

The present interest in the interaction of transverse jets is to provide a means of improving the analysis and computation of supersonic combustor flows. The challenge to the complete analysis of the flowfield resulting from the transverse injection in a supersonic stream is to develop a means to handle the elliptic TJI flow region in such a way that will eliminate the need to explicitly solve the elliptic form of the conservation equations. The basic concept of the present approach is to transform the TJI region in a physically compatible way that can be computationally coupled with a parabolic flow solution technique. To implement this coupled solution, the physics of the interaction are modeled such that nearly parallel flow conditions are obtained that are

representative of the initial mixing of the transverse jet. These flow conditions of the TJI region provide the input needed to start the numerical solution of the equations that describe the downstream parabolic flow in a supersonic combustor. Results of these computations are predictions of the details of the fuel mixing and reaction downstream of the injection region and integral parameters of the overall mixing. The present work will examine this coupled solution approach to the problem of analyzing the flow downstream of a transverse fuel jet in supersonic combustion ramjets. The primary purpose of this paper is to present a two-dimensional mathematical model of the TJI flow region that can be used to initialize a detailed two-dimensional calculation using an existing parabolic-flow computer code. An initial evaluation of the model is obtained by comparing the computed results with some existing supersonic combustion data.

Investigations of the interaction between a transverse jet and a supersonic mainstream flow have attempted to identify the principal parameters characterizing the scale of the resulting aerodynamic effects. The most commonly used scaling parameter is the jet penetration height, generally defined as the location of the jet Mach disk shock.[1-5] Where details of the near-jet flow region were not available, jet penetration has been characterized by the downstream trajectories of the height of maximum and zero concentration of the injectant.[5-9] Simple models of the TJI flow have been formulated to obtain the size of the solid body that will produce an equivalent disturbance.[3,6,10] The most widely used scaling parameter is a theoretical jet penetration height[3] derived by replacing the jet flow with a quarter-sphere body. In a more sophisticated analysis,[1] the path of the jet centerline was obtained by assuming that the injected gas could be treated as a circular cylinder. Other analyses have modeled the transverse jet interaction by establishing the size of the solid body that produces an equivalent bow shock structure. Shock-shape data for sonic hydrogen injection from a discrete orifice injector[1] compared favorably with a model[11] which gives the bow shock coordinates for flow over a spherical-nosed body.

Studies of the details of the mixing process of transverse jets have been conducted in a number of experimental investigations for both inert[1,5,7-9,12,13] and chemically reactive[14,15] flows over a wide range of conditions and injector configurations. These data have provided correlations of the trajectories of the jet penetration and location of peak concentration as functions of downstream distance and injection parameters. In addition, the injectant composition profiles have been found to have the shape of a Gaussian-type function[5,9] and to be similar at the various downstream stations. Composition data profiles also have been used to obtain integral parameters such as the fraction of injectant mixed to a reactable level. Analysis of these results has led to correlations of the rate of mixing with downstream distance[9] for hydrogen injected from discrete orifices into a Mach 4 airstream. This mixing parameter, in conjunction with a one-dimensional flow theory, has been used, with moderate success, to aid the analysis and interpretation of reacting flow data.[14,15] Of particular interest to the present analysis are the data and integral results of Ref. 15 which will be used to obtain an initial evaluation of the proposed transverse jet model for a particular application.

Flowfield Model

The objective of this analysis is to model the interaction of a transverse jet in a supersonic stream so as to obtain the flow properties that can be input into a detailed computation of a supersonic combustor flow. The principal aerodynamic features[1,2] of the TJI are presented in Fig. 1. The development of a flow model requires some means of handling the flow separation zones immediately upstream and downstream of the injector, the separation and bow shock waves caused by the jet blockage, and the jet Mach disk shock. The separation shock is a planar (in the two-dimensional case) oblique shock.

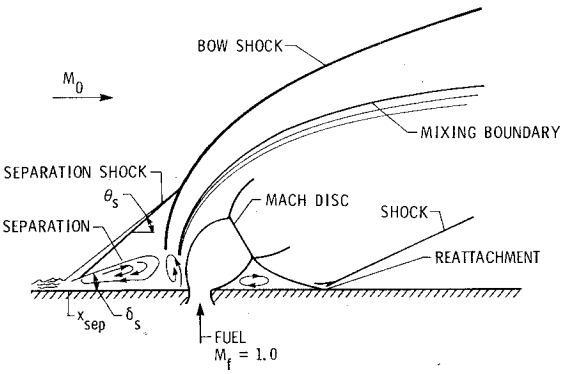

Fig. 1 Aerodynamic features of transverse jet interaction.

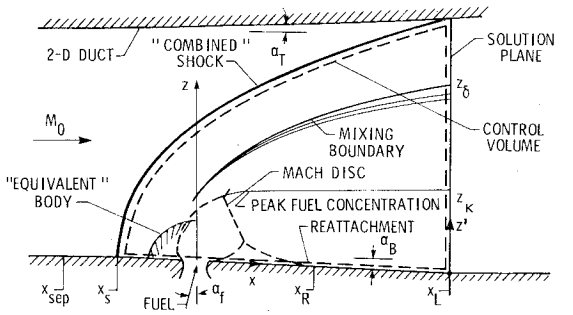

Fig. 2 Flow model of transverse jet interaction.

In general, as for the case of an unbounded mainstream, the bow shock produces no net turning of the flow and approaches a Mach line at large distances from the jet. In the separated flow region downstream of the injector, wall pressure data[3,16] indicate that the flow expands rapidly and recompresses to approximately the pressure in the undisturbed mainstream at the reattachment point. The jet Mach disk shock occurs as the jet fluid expands from sonic conditions and is characteristic of the scale of the jet penetration.[1-3]

Considering these pertinent features of the TJI flowfield, it is assumed that the flow in the vicinity of a two-dimensional injector can be represented by the two-dimensional model presented in Fig. 2. The flow is confined in a duct with walls that diverge at small angles α_T and α_B. The hydrogen fuel jet is injected at an angle α_f from the vertical. The leading shock wave is assumed to be a linear combination of the separation and bow shocks. This means that, at large distances from the injector, the turning imparted to the flow is equal to that of a wedge with the same shock angle as the upstream separation region. At the downstream location where the combined shock intersects the opposite wall, the solution plane is taken. This surface, along with the combined shock and injection wall, define the model control volume, shown by the broken lines in Fig. 2. Assuming that the coordinates of the combined shock and the pressure distribution along the injection wall are known, the conservation equations can be written for the model control volume to relate the flow properties in the solution plane to the initial conditions of the jet and mainstream.

Governing Equations

Starting with the divergence form of the conservation equations and assuming that the flow is steady, that body forces, conduction, and radiation are negligible, that no chemical reactions occur in the binary mixture of fuel and mainstream, and that diffusive transport is small compared with convection, the equations can be reduced to the

following:

Mass:

$$\oint_s \rho v_i n_i \mathrm{d}S = 0 \tag{1a}$$

Species:

$$\oint_s \rho v_i \kappa n_i \mathrm{d}S = 0 \tag{1b}$$

Momentum:

$$\oint_s (\rho v_i v_j - P_{ij}) n_i \mathrm{d}S = 0 \tag{1c}$$

Energy:

$$\oint_s (\rho e v_i - v_j P_{ij}) n_i \mathrm{d}S = 0 \tag{1d}$$

where the n_i are unit normal vectors directed outward from each surface, and P_{ij} is the general stress tensor defined as:

$$P_{ij} = -p\delta_{ij} + \mu_o (\partial v_i/\partial x_j + \partial v_j/\partial x_i) \tag{2}$$

Further, assuming that the shear stress components of P_{ij} are negligible in comparison with the pressure except on the duct walls, Eq. (1) can be integrated over the surfaces of the control volume to obtain, per unit width of duct:

Mass:

$$\int_0^{h_2} \rho_2 V_2 \cos\delta_2 \mathrm{d}z' = (1+f)\dot{m}_0 \tag{3}$$

Species:

$$\int_0^{h_2} \rho_2 V_2 \kappa \cos\delta_2 \mathrm{d}z' = f\dot{m}_0 \tag{4}$$

Streamwise momentum:

$$\int_0^{h_2} (\rho_2 V_2^2)\cos^2\delta_2 \mathrm{d}z' + \int_0^{h_2} p_2 \mathrm{d}z' = \rho_0 V_0^2 h_0 + p_0 (h_0 - x_{LG}\tan\alpha_T) - S_F(\cos\alpha_B + \cos\alpha_T) + F_J \sin\alpha_f - F_w \tan\alpha_B \tag{5a}$$

Transverse momentum:

$$\int_0^{h_2} (\rho_2 V_2^2)\sin\delta_2\cos\delta_2 \mathrm{d}z' = F_J\cos\alpha_f + F_w - p_0 x_{LG} - S_F(\sin\alpha_T + \sin\alpha_B) \tag{5b}$$

Energy:

$$\int_0^{h_2} (\rho_2 V_2) H_2^o \cos\delta_2 \mathrm{d}z' = (fH_f^o + H_0^o)\dot{m}_0 \tag{6}$$

Additionally, it has been assumed in deriving Eqs. (3-6) that α_T is small so that any change (due to the expansion of the duct) in the mainstream Mach number approaching the combined shock is negligible.

The energy Eq. (6) can be reduced to an algebraic relation between static temperature and velocity in the solution plane by assuming that convection dominates the energy transport. This assumption implies that the local stagnation enthalpy is directly related to the composition

$$H_2^o = (1-\kappa)H_0^o + \kappa H_f^o \tag{7}$$

which can be shown to satisfy Eq. (6). The resulting energy equation is

$$H_2(T) + V_2^2/2 = H_2^o \tag{8}$$

Equations (3-5) and (8), along with the equation of state provide six equations in the six unknowns T, V, p, κ, δ and (ρV). The mass flux (ρV) is taken as an unknown because it appears in the integrals of Eqs. (3-5) and a functional form of the shape of the (ρV) profile is more readily obtained from mixing data. It is convenient to write the equation of state in terms of the unknown parameters, to obtain

$$V = (\rho V) R^o T/p\mu \tag{9}$$

These equations cannot be solved in their present form without knowing something about the profiles in the solution plane of the flow variables—p, (ρV), κ, and δ—that appear in the integral terms. For the case of a uniformly mixed flow, all of these variables are constant, and the six equations can be readily solved for the state of the final mixture. The goal of the TJI model, however, is to obtain profiles of the flow properties in the solution plane. To achieve this goal, nondimensional profiles of the four flow variables will be determined based on available mixing data for an unconfined, nonreacting flow. Each of the profile shapes will be represented by a mathematical function containing only one unknown that is representative of the magnitude of the flow variable. The integral terms in Eq. (3-5) can then be evaluated in terms of these unknowns and the equations solved to determine the actual profiles. First, however, the coordinates of the combined shock are needed to define the size of the control volume and to provide boundary conditions at the opposite wall for the assumed profile shapes.

Shock Solution

The coordinates of the combined shock used in the TJI model in Fig. 2 are obtained from the relation[11]

$$\frac{x}{d} = -\frac{x_s}{d} + \cot^2\theta_s \left\{ \left[R_S^2 + \left(\frac{z}{d}\right)^2 \tan^2\theta_s \right]^{1/2} - R_s \right\} \tag{10}$$

where:

$$\frac{x_s}{d} = \frac{R_B}{d}\left(1 + \frac{D}{R_B}\right) \text{ and } R_S = \frac{R_C}{R_B}\frac{R_B}{d}$$

For a spherical-nosed body[11]

$$R_C = 1.143 \exp[0.54/(M_0 - 1)^{1.2}] R_B \tag{11}$$

$$D/R_B = 0.143 \exp(3.24/M_0^2) \tag{12}$$

where R_B/d is the radius of the equivalent body. Good agreement between Eq. (10) and measured shock coordinates was obtained for hydrogen jets[1] when the radius of the jet equivalent body was taken as the height of the midpoint of the jet Mach disk. For discrete orifice jets, the location of the Mach disk has been correlated[2] as the square root of the ratio of jet pressure and an effective back pressure,

$$R_B/d = (p_f/p_B)^{1/2} \tag{13}$$

The local shock angle, θ is

$$\tan\theta = \left[R_S^2 \Big/ \left(\frac{z}{d}\right) + \tan^2\theta_s \right]^{1/2} \tag{14}$$

where θ_s is the angle the shock wave approaches at large distances from the body and, therefore, represents the net turning imparted to the mainstream flow by the jet disturbance. For a free jet in an unconfined mainstream and the bow shock shown in Fig. 1, θ_s is the mainstream Mach angle. For the present case of the assumed combined shock with a net turning at large z/d equal to that of the upstream separation zone, θ_s is the separation shock angle.

In order to obtain the combined shock coordinates, it is first necessary to determine the separation shock angle θ_s. This is done by assuming that 1) the pressure on the injection wall upstream of the jet ($x<0$) is the pressure behind the combined shock, and 2) the pressure force on the upstream wall is the same for the separation and bow shocks (Fig. 1) and the combined shock (Fig. 2). These assumptions imply that

$$p_{sep}(x_{sep}-x_{s,bow})+\int_{-x_{s,bow}}^{0} p_{bow}\,dx=\int_{-x_s}^{0} p_s\,dx \qquad (15)$$

where $x_{s,bow}$ is the shock standoff distance for the bow shock at a Mach number M_1 downsteam of the separation shock. Pressures p_s and p_{bow} are the local values downstream of the combined shock and bow shock, respectively. The separation distance is $x_{sep}=H_s/\tan\delta_s$ where H_s is the height of the separation zone, arbitrarily chosen as half the equivalent body radius, $H_s=R_B/2$. This choice is supported by the results of Ref. 1 in which a displacement parameter β was used to locate the computed shock above the injection surface to match the data. This parameter was graphically correlated with the equivalent body radius and ranged from $\beta/R_B=0.52$ to 0.61. With these assumptions, Eq. (15) can be solved for θ_s and the coordinates of the combined shock determined.

Wall Pressure Distribution

The assumed pressure distribution on the injection wall is presented in Fig. 3. Upstream of the jet ($x<0$) the wall pressure is assumed to be the local pressure behind the assumed combined shock as discussed in the previous section. Downstream of the jet ($x>0$) the assumed wall pressure distribution is based on data reported in experimental studies for both discrete orifice and slot jets.[2,3,16,17] Typical of these data are the wall pressures[16] shown in the inset of Fig. 3. Downstream of the jet, these data indicate a rapid expansion followed by a recompression to approximately the mainstream pressure at the reattachment point. Based on these observations, the TJI model assumes a wall pressure distribution downstream of the jet ($x>0$) that has expanded to the reciprocal of the combined shock local pressure at the jet location followed by a linear recompression to the level in the undisturbed mainstream at the reattachment point. It is additionally assumed, based on the data, that the distance to reattachment is equal to the upstream separation distance.

Assumed Profile Shapes in Solution Plane

The key feature of the proposed TJI model is the assumed functional form of the profiles of the fuel mass fraction, the total mass flux, static pressure, and local flow angle. The nondimensional profile of fuel mass fraction is given in Fig. 4 with data[9] at a downstream station of 7 jet diameters. These data are typical of other mixing studies reported and were shown to be well represented by a Gaussian function[5,9] of the form

$$\kappa=\kappa_{max}\exp(-A_k\hat{Z}^2) \qquad (16)$$

Here κ_{max} is the local peak concentration and the nondimensional coordinate $\hat{Z}$ is

$$\hat{Z}=C_u(z/z_\kappa-1),\quad z>z_\kappa \qquad (17)$$

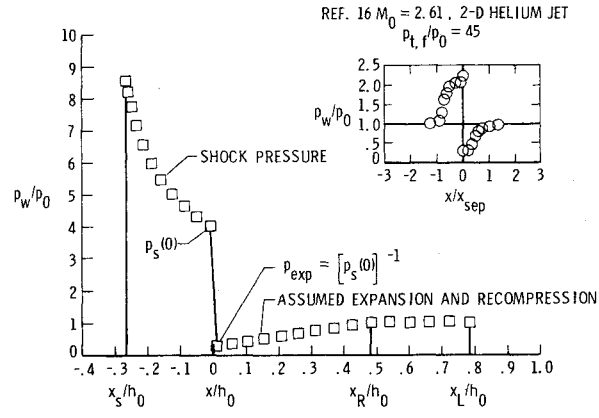

Fig. 3 Assumed wall pressure distribution.

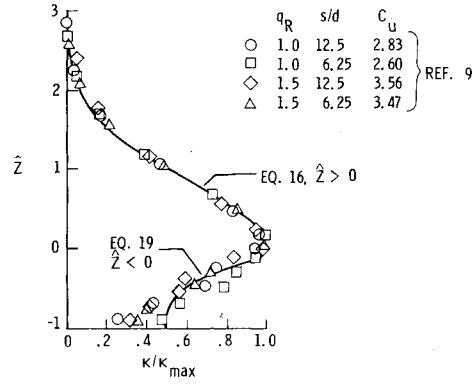

Fig. 4 Comparison of assumed fuel mass fraction profile with nonreacting data.

The rate of decay of the profile, C_u is defined for $z>z_\kappa$ as

$$C_u=\left(\frac{z_\kappa}{z_\delta-z_\kappa}\right)\left[-\frac{\ell n\kappa_\delta}{A_k}\right]^{1/2} \qquad (18)$$

For the region between the injection wall and the peak concentration, $z<z_\kappa$, $C_u=1$, and the profile has the form

$$\kappa/\kappa_{max}=(1-\kappa_w/\kappa_{max})\exp(A_{ko}\hat{Z}^2)+\kappa_w/\kappa_{max},\quad z\le z_\kappa \qquad (19)$$

where $\kappa_w=0.5\ \kappa_{max}$ is the value of κ on the wall, and $A_{ko}=\ell n(\kappa_\delta/(\kappa_{max}-\kappa_w))$. The assumed profile shape for $z<z_\kappa$ is modified from the simple Gaussian shape used in Ref. 9 to give a better fit of the data profiles near the injector.

To use the assumed profiles, Eqs. (16) and (19), the locations of the local peak concentration z_κ and the edge of the mixing region z_δ are needed. Correlations for these penetration heights have been derived from several experimental investigations.[1,5,7-9,12,13] Data presented in Ref. 5 indicate that the peak concentration can be represented by the location of the top of the Mach disk (Fig. 2), which was correlated to be about 1.5 times the Mach disk midpoint heights given by Eq. (13). The location of the peak concentration is, then,

$$\frac{z_\kappa}{d}=1.5\left(\frac{\gamma_0 M_0^2}{\gamma_f M_f^2}\frac{p_0}{p_B}q_r\right)^{1/2} \qquad (20)$$

For data measurements near the injection of a hydrogen jet of $M_0=2.72$,[1] the edge of the mixing region has been correlated by

$$\frac{z_\delta}{d}=1.68\left(\frac{M_0}{M_f}\right)^{1/2}q_r^{1/2}\left(\frac{x}{d}\right)^{0.0866} \qquad (21)$$

Data[9] for a sonic hydrogen jet at $M_0 = 4.03$ were correlated for $x/d > 7$ by

$$z_\delta/d = 3.87 q_r^{0.3} (x/d)^{0.143} \quad (22)$$

Differences in the correlating constants in these two equations may be due to differences in flow conditions, such as the turbulent boundary layer thickness on the injection wall.[9] Assuming that the effect of mainstream Mach number as given in Eq. (21) is correct, Eq. (22) can be written, for a sonic hydrogen jet, as

$$z_\delta/d = 1.93 M_0^{1/2} q_r^{0.3} (x/d)^{0.143} \quad (23)$$

For lack of a means to justify the use of one correlation over the other, the edge of the mixing region is taken as the average value given by Eqs. (21) and (23). The only remaining unknown in the fuel concentration profile is the value of the peak concentration κ_{max}, which can be found from solution of the species conservation equation.

The profile shape of the total mass flux was obtained by reviewing mixing data[7,9,12] for sonic hydrogen jets in an unconfined $M_0 = 4.03$ mainstream. Selected data from Ref. 9 are shown in Fig. 5. These data have been nondimensionalized by the mass flux at the edge of the mixing region. A good fit to the data in the mixing region ($z < z_\delta$) was obtained by the Gaussian-type function

$$R(Z) = (1 - C_R) \exp\left[-A_R \left(1 - \frac{Z}{Z_\delta}\right)^2\right] + C_R, \quad Z < Z_\delta \quad (24)$$

Between the edge of the mixing region and the opposite wall ($Z > Z_\delta$) the mass flux varies from R_δ to the value behind the combined shock R_L. For the TJI model, a quadratic varation was assumed subject to these constraints and with a slope equal to that of Eq. (24) at $Z = Z_\delta$. For $Z > Z_\delta$, the mass flux profile is

$$R(Z) = 1 + \left(\frac{Z - Z_\delta}{1 - Z_\delta}\right)^2 \left(\frac{R_L}{R_\delta} - 1\right), \quad Z > Z_\delta \quad (25)$$

The only unknown in Eqs. (24) and (25) is the mass flux at the edge of the mixing region $R_\delta = (\rho V)_\delta$, which can be found from the conservation of mass.

The static pressure profile in the solution plane was assumed to vary as a second-order polynomial from the known values on the injection surface $p_w = p_0$ and behind the combined shock at the opposite wall, p_L. The needed third constraint was obtained by defining the mean pressure force over the solution plane as

$$p_m = \int_0^1 p_2(Z)\,dZ \quad (26)$$

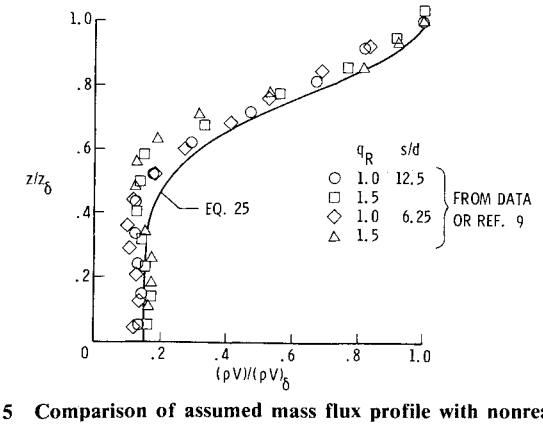

Fig. 5 Comparison of assumed mass flux profile with nonreacting data.

The resulting pressure profile is then

$$p_2 = p_w + Z(3Z-4)p_w + Z(3Z-2)p_L + 6Z(1-Z)p_m \quad (27)$$

The only unknown is the mean pressure p_m which can be found from the solution of the momentum equations.

In a similar way, the local flow angle is assumed to be represented by a second-order polynomial, under the constraints imposed by the injection wall at an angle α_B and the combined shock at the opposite wall with the flow angle δ_L. These constraints give

$$T(Z) \equiv \frac{\tan\delta_2}{\tan\delta_L} = (1-c)Z + cZ^2 + (1-Z)\tan\alpha_B/\tan\delta_L \quad (28)$$

The unknown coefficient c is found by defining the mean flow angle δ_m such that

$$\tan\delta_m \int_0^1 (\rho V)_2 dZ = \tan\delta_L \int_0^1 (\rho V)_2 T(Z)\,dZ \quad (29)$$

For a given value of the mean flow angle, Eq. (29) can be solved iteratively for c and the flow angle profile obtained from Eq. (28). The unkown here is the mean flow angle, which is obtained from the solution of the transverse momentum equation.

Through the preceding assumptions, each of the unknown profiles has been replaced by a single unknown parameter that defines the magnitude of the profile $-\kappa_{max}$, $(\rho V)_\delta$, p_m, $\tan\delta_m$, respectively. Equations (3-5) can now be reduced to a set of four algebraic equations and solved iteratively.

Reduction of Equation and Solution Procedure

Defining nondimensional variables as $(\bar{\rho V}) = (\rho V)/(\rho V)_0$, $\bar{V} = V/V_0$, $\bar{p} = p/p_0$, $Z = z'/h_2$, $\bar{h}_2 = h_2/h_0$, and $\bar{\kappa} = \kappa/\kappa_{max}$, and substituting the assumed profile functions, Eqs. (3-5) reduce to

Mass:

$$\bar{h}_2 \bar{R}_\delta \int_0^1 R\cos\delta_2\,dZ = 1 + f \quad (30)$$

Species:

$$\bar{h}_2 \bar{R}_\delta \kappa_{max} \int_0^1 R\bar{\kappa}\cos\delta_2\,dZ = f \quad (31)$$

Streamwise momentum:

$$\bar{h}_2(\gamma M_0^2)\bar{R}_\delta \int_0^1 R\bar{V}\cos^2\delta_2\,dZ + \bar{h}_2\bar{p}_m = 1 + \gamma M_0^2 + \bar{x}_{LG}\tan\alpha_T - \bar{S}_{Fx} - \bar{F}_{Jx} - \bar{F}_{wx} \quad (32)$$

Transverse momentum:

$$\bar{h}_2(\gamma M_0^2)\bar{R}_\delta \int_0^1 R\bar{V}\cos\delta_2\sin\delta_2\,dZ = \bar{F}_{JZ} + \bar{F}_w - X_{LG} - \bar{S}_{FZ} \quad (33)$$

The solution of Eqs. (30-33) is obtained by iterating on the unknown parameters $\bar{p}_m$ and $\tan\delta_m$. First, the combined shock and wall pressure are obtained from the given jet and mainstream condition. Initial guesses of $\bar{p}_m$ and $\tan\delta_m$ are obtained from a one-dimensional solution of the flow, neglecting the shock effects. The locations of the peak concentration and mixing boundary are found from Eqs. (20), (21), and (23). Next, an iteration is begun in which the pressure and flow angle profiles are computed. Equations (30) and (31) are solved for R_δ and κ_{max}, respectively, and the solution profiles of κ and (ρV) are computed from Eqs. (16),

(19), (24), and (25). The energy Eq. (8) is solved with Eq. (9) for the velocity and temperature at each point in the profiles. Finally, the momentum imbalance of Eqs. (32) and (33) is checked and corrections to $\tilde{p}_m$ and $\tan\delta_m$ made using a Newton-Raphson procedure.

TJI Model Results

Some typical results of the TJI model are presented in Figs. 6 and 7. These results were obtained at flow conditions representative of supersonic combustor flow, based on the experimental investigation presented in Ref. 15. The flow is confined within a slightly diverging duct with the mainstream test gas at $M_0 = 2.7$, $T_{t,0} = 2200$ K, and $p_0 = 0.0714$ MPa and hydrogen fuel at $T_{t,f} = 805$ K, $q_r = 3.0$, and sonic velocity. Figure 6 gives the nondimensional fuel mass fraction and total mass flux profiles, assumed across the duct height in the solution plane, as obtained by the model. Figure 7 gives the solution plane profiles of density, pressure, temperature, and velocity nondimensionalized by the mainstream values.

Comparison with Data

The impetus behind the development of a model of the TJI was to establish such profile information and use it to initiate a detailed computational procedure of supersonic combustor flows. Results from the detailed computations could then be compared with data for transverse fuel injection tests. An existing computer code, called SHIP (Supersonic Hydrogen Injection Program)[18] was used for this purpose.

SHIP Computer Code

The SHIP computer program[18] uses a finite difference, implicit, forward-matching numerical procedure to compute the combustion of hydrogen in a supersonic airstream. The boundaries of the computational domain may be free, symmetry planes, or wall surfaces. Included in the program is a two-equation turbulence model which uses the turbulent kinetic energy and dissipation to determine the effective turbulent viscosity. The basic three-dimensional parabolic flow program has been evaluated, with generally good results, for several subsonic and supersonic, turbulent, reacting and nonreacting flow problems.[19] Chemical reactions in SHIP are handled through the equilibrium hydrogen/oxygen reaction with nitrogen assumed inert. For the purpose of an initial evaluation of the TJI model, and since the available data chosen for comparison[15] indicated only the extent of accomplished mixing, the SHIP code was modified assuming completely reacted products.

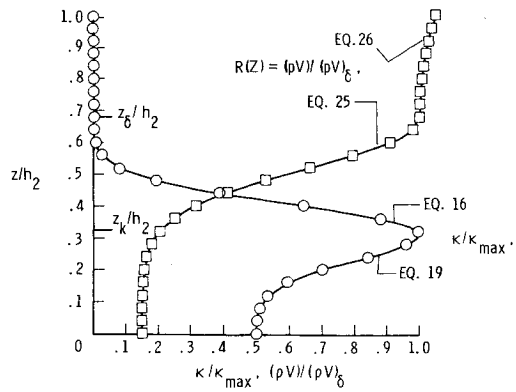

Fig. 6 Profiles of fuel mass fraction and total mass flux in solution plane.

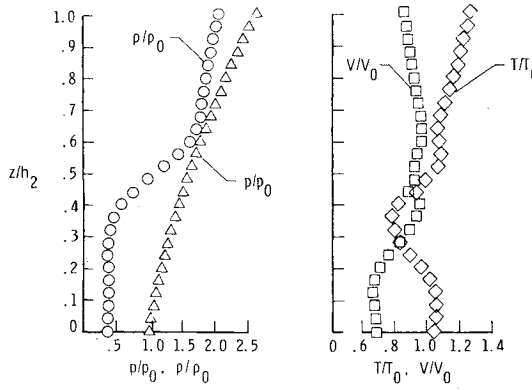

Fig. 7 Profiles in solution plane of the TJI model.

In addition to the input profiles from the TJI model—static temperature and pressure, streamwise and transverse velocities, and fuel mass fraction—it was necessary to specify initial values of the turbulent kinetic energy (TKE) and turbulence dissipation. This was accomplished by assuming that the initial turbulent viscosity can be approximated by the Prandtl mixing length hypothesis. Such a procedure has been used[20] to relate the TKE to the local gradient of streamwise velocity V_x and a characteristic length scale. The result is

$$K^{1/2} = L_m(\partial V_x/\partial z)C_D^{1/2} \tag{34}$$

where $C_D = 0.09$ is a constant in the two-equation turbulence model used in SHIP. The choice of an appropriate length scale is arbitrary. For the purpose of using the TJI model, the length scale was chosen as Z_δ, the extent that the injected hydrogen fuel has spread across the duct. The mixing length L_m is taken as $C_D Z_\delta$ is to be consistent with the turbulence model used in SHIP.

Theory and Data Comparisons

This section will present comparisons of the data with the results obtained from the SHIP code using the TJI model to initialize the calculation. In interpreting these comparisons, several factors need to be kept in mind regarding the assumptions and approximations involved. The TJI model used a combined shock that was assumed to be two-dimensional based upon an equivalent body of the jet penetration. As such it did not include any effect the jet disturbance may have on the upstream flow. In addition, the turbulence model used in the SHIP code is based on two-dimensional shear flows and may not be suitable for flows of the type under consideration. The need to hypothesize initial values of the turbulence is another uncertainty. The TJI model is two-dimensional, but was developed semi-empirically based on profiles for a discrete orifice in a nonreacting, unconfined flow. In a confined, reacting flow, data profiles would likely be different; however, the author is unaware of any detailed profile data near a transverse jet for such flows. Since the intent is to apply the nonreacted profiles of the TJI model to the calculation of reacting flow, it was necessary to react the initial profiles input to the SHIP code. This initial reaction was performed by first finding the completely reacted products at each grid point. The reaction temperature was computed to conserve energy and the reaction pressure field found to conserve mass. The philosophy of the theory-data comparisons at this stage in the development of the TJI model was to evaluate the potential usefulness of this approach to the analysis of a general three-dimensional supersonic combustion problem. The goal was to obtain reasonable agreement in the trends of the data and theory.

The experimental data compared with the SHIP computations using the TJI model were obtained for the supersonic combustion of transversely injected hydrogen in a two-dimensional duct.[15] The following comparisons present some of the data in a form modified from that of the original paper. Two of the test conditions presented in Ref. 15 will be used to compare with the theoretical results. Case A had injectors of 0.506 cm diameter with the hydrogen fuel heated to ap-

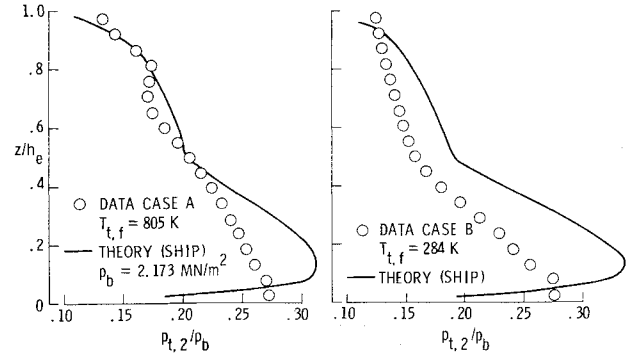

Fig. 8 Comparison of pitot pressure profiles in the data survey plane with theory.

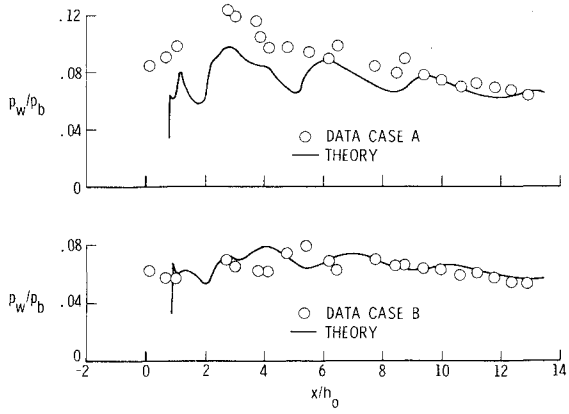

Fig. 9 Comparison of pressure distributions on the injection wall with theory.

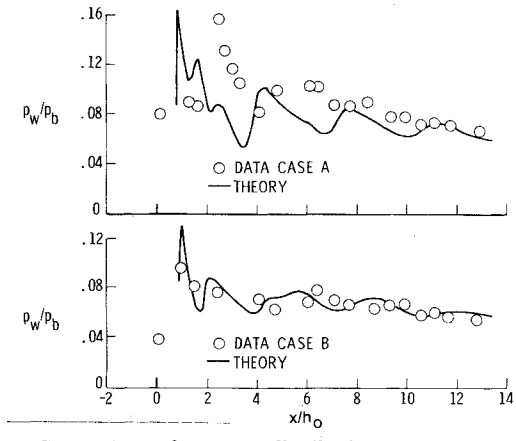

Fig. 10 Comparison of pressure distributions on the opposite wall with theory.

proximately 805 K. Case B used the same injections with ambient temperature (284 K) fuel. Estimated dynamic pressure ratios for the two cases are $q_r = 3.0$ and 1.73, respectively. Note that for these comparisons the fuel is injected from the upper wall. The comparisons of the average pitot pressure data profiles with the SHIP theory are presented in Fig. 8, with the pitot pressures nondimensionalized by the stagnation pressure of the test gas (mainstream), p_b. For both of these cases, the general shape of the theory profiles are very similar to the data, exhibiting a lower level in the upper, fuel-rich region. The inflection of the theoretical pitot profiles near the midpoint of the flow occurs at the location where the fuel-test gas mixture is locally stoichiometric. For case A, the agreement of the data and

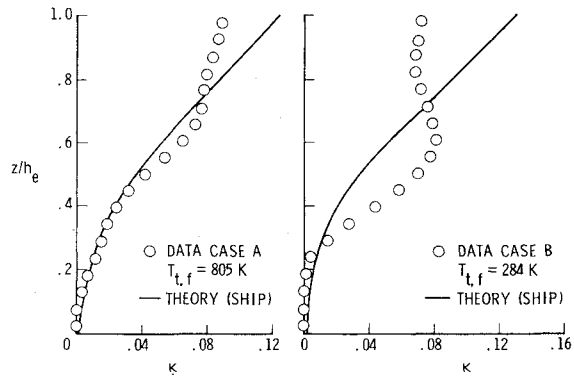

Fig. 11 Comparison of fuel mass fraction profiles in the data survey plane with theory.

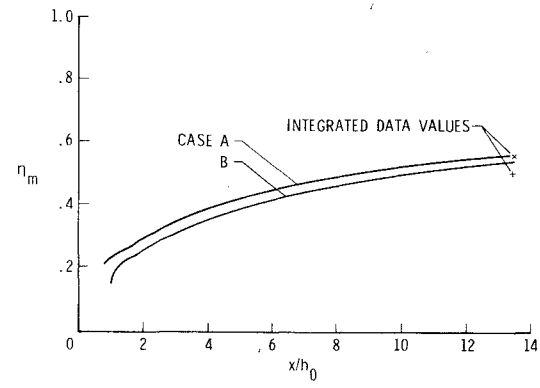

Fig. 12 Comparison of the mixing parameter distribution with integrated data values.

theory in the upper half of the flow is very good. For case B, the magnitude of the theory is about 15-20% too high. This difference in magnitude is certainly affected by the higher level of computed static pressure of the SHIP results (approximately 10%) relative to the uniform value assumed in reducing the survey plane data.

Figures 9 and 10 present comparisons of the wall pressure data and the SHIP predictions. Generally, the agreement is good in trend, but the magnitude is off in the near injector region. The oscillations in the theoretical pressure distribution from SHIP physically match those observed in the data, and result from the reversal of the transverse component of velocity at the duct walls. In this way the pressure oscillations from SHIP approximate the location of the shock waves reflecting down the duct. Differences in the magnitude of the data and theory pressures near the injector are also likely due to the application of the TJI model based on nonreacting free jet data to a reacting flow. Reaction occurring in the transverse jet interaction would raise the pressure on the injection wall, as indicated by the data for case A (Fig. 10), whereas the TJI model assumes the pressure is returned to that of the undisturbed mainstream. The overall agreement of the pressures is considered good, particularly with regard to the location of the local peaks.

In Fig. 11, the average fuel mass fraction data are compared with the SHIP calculation for cases A and B. The agreement for the hot fuel (case A) is quite good, except near the injection wall where the average data are mixed to a mass fraction value about three-fourths of the theory value. For cold fuel (case B), the agreement is not as good, even though the profiles do exhibit about the same spread of the fuel across the duct. The difference in the quantitative agreement between the theory and data comparisons presented is likely due to a combination of the assumptions and approximations inherent to the TJI model and the SHIP code. Another likely factor contributing to these differences is the two-dimensional

nature of the SHIP calculation when the data are in reality three-dimensional.

As a final comparison of the theory with data, the distribution of the mixing efficiency parameter with downstream distance is presented in Fig. 12. The solid lines are the SHIP theory results for cases A and B and are compared with the overall values obtained from the integration of the data. The attractive implication for scramjet engine design is that even though the details of the fuel mass fraction profiles might not be accurately predicted by the theory, the predicted level of accomplished mixing can be good. Considering the uncertainties inherent in the TJI model, this overall agreement between integrated data and theory is encouraging. The TJI model appears to offer attractive potential as a near-term solution to the transverse flowfield problem.

Concluding Remarks

A two-dimensional, nonreacting flow model of the injection of a transvese jet has been developed. The model is based on profile shapes of the flow parameters as observed from experimental data profiles taken downstream of a transverse hydrogen jet in an unconfined, nonreacting flow. Results of detailed calculations have been compared with available fuel mass fraction and pitot pressure data at the exit of the combustion duct to check the ability of the proposed model to provide initial conditions for practical two-dimensional combustor flows involving transverse fuel injection. Generally good agreement was obtained, particularly with respect to the integrated extent of mixing accomplished at the duct exit.

Considering the difficulty of a completely analytical solution for the transverse jet interaction, particularly in a reacting flow environment, the two-dimensional mathematical model presented here does an adequate job of beginning a detailed two-dimensional computation of a supersonic reacting flow. The assumptions and approximations included in the development of the transverse jet model could be improved to include reaction, pending the availability of the necessary profile data. However, the overall good results obtained in this initial evaluation of the model are very encouraging as to its use in the computation of practical supersonic combustor flow configurations.

References

[1] Orth, R. C., Schetz, J. A., and Billig, F. S., "The Interaction and Penetration of Gaseous Jets in Supersonic Flow," NASA CR-1386, July 1969.

[2] Werle, M. J., Driftmyer, R. T., and Shaffer, D. G., "Two-Dimensional Jet Interaction with a Mach 4 Mainstream," U.S. Naval Ord. Lab., NOLTR-70-50, May 1970.

[3] Spaid, F. W., Zukowski, E. E., and Rosen, R., "A Study of Secondary Injection of Gases into Supersonic Flow," Jet Propulsion Lab., Tech. Rept. 32-834, Aug. 1966.

[4] Sterrett, J. R. and Barber, J. B., "A Theoretical and Experimental Investigation of Secondary Jets in a Mach 6 Free Stream with Emphasis on the Structure of the Jet and Separation Ahead of the Jet," *Separated Flows, Pt. II, AGARD Conference Proceedings*, No. 4, May 1966, pp. 667-700.

[5] Cohen, L. S., Coulter, L. J., and Egan, W. J., Jr., "Presentation and Mixing of Multiple Gas Jets Subjected to a Cross Flow," *AIAA Journal*, Vol. 9, April 1971, pp. 718-724.

[6] Billig, F. S., Orth, R. C., and Lasky, M., "A Unified Analysis of Gaseous Jet Penetration," *AIAA Journal*, Vol. 9, Sept. 1971, pp. 1048-1058.

[7] Torrence, M. G., "Concentration Measurements of an Injected Gas in a Supersonic Stream," NASA TN D-3860, April 1967.

[8] Rogers, R. C., "A Study of the Mixing of Hydrogen Injected Normal to a Supersonic Airstream," NASA TN D-6114, March 1971.

[9] Rogers, R. C., "Mixing of Hydrogen Injected from Multiple Injectors Normal to a Supersonic Airstream," NASA TN D-6476, Sept. 1971.

[10] Werle, M. J., "A Critical Review of Analytical Methods for Evaluating Control Forces Produced by Secondary Injection," U.S. Naval Ord. Lab., NOLTR 68-5, Jan. 1968.

[11] Billig, F. S., "Shock-Wave Shapes Around Spherical and Cylindrical-Nosed Bodies," *Journal of Spacecraft and Rockets*, Vol. 4, June 1967, pp. 822-823.

[12] Torrence, M. G., "Effect of Injectant Molecular Weight on Mixing of a Normal Jet in a Mach 4 Airstream," NASA TN D-6061, Jan. 1971.

[13] Wagner, J. P., Cameron, J. M., and Billig, F. S., "Penetration and Spreading of Transverse Jets of Hydrogen in a Mach 2.72 Airstream," NASA CR-1794, March 1971.

[14] Rogers, R. C. and Eggers, J. M., "Supersonic Combustion of Hydrogen Injected Perpendicular to a Ducted Vitiated Airstream," AIAA Paper 73-1322, Nov. 1973.

[15] Rogers, R. C., "Influence of Fuel Temperature on Supersonic Mixing and Combustion of Hydrogen," AIAA Paper 77-17, Jan. 1977.

[16] Spaid, F. W. and Zukowski, E. E., "A Study of the Interaction of Gaseous Jets from Transverse Slots with a Supersonic External Flow," *AIAA Journal*, Vol. 6, Feb. 1968, pp. 205-212.

[17] Zakkay, V., Calarese, W., and Sakell, L., "An Experimental Investigation of the Interaction Between Transverse Sonic Jets and a Hypersonic Stream," *AIAA Journal*, Vol. 9, April 1971, p. 674-682.

[18] Markatos, N. C., Spalding, D. B., and Tatchell, D. G., "Combustion of Hydrogen Injected into a Supersonic Airstream (The SHIP Computer Program)," NASA CR-2802, April 1977.

[19] Pan, Y. S., "Evaluation of the Three-Dimensional Parabolic Flow Computer Program SHIP," NASA TM-74094, Jan. 1978.

[20] Evans, J. S., Schexnayder, C. J., Jr., and Beach, H. L., Jr., "Application of a Two-Dimensional Parabolic Computer Program to Prediction of Turbulent Reacting Flows," NASA TP-1169, March 1978.